




Haptic Intracorporeal Palpation Using a Cable-Driven Parallel Robot: A User Study

Arianna Saracino, *Student Member, IEEE*, Timo J. C. Oude-Vrielink ,
Arianna Menciassi, *Senior Member, IEEE*, Edoardo Sinibaldi , *Member, IEEE*,
and George P. Mylonas , *Member, IEEE*

Abstract—Objective: Intraoperative palpation is a surgical gesture jeopardized by the lack of haptic feedback which affects robotic minimally invasive surgery. Restoring the force reflection in teleoperated systems may improve both surgeons' performance and procedures' outcome. **Methods:** A force-based sensing approach was developed, based on a cable-driven parallel manipulator with anticipated seamless and low-cost integration capabilities in teleoperated robotic surgery. No force sensor on the end-effector is used, but tissue probing forces are estimated from measured cable tensions. A user study involving surgical trainees ($n = 22$) was conducted to experimentally evaluate the platform in two palpation-based test-cases on silicone phantoms. Two modalities were compared: visual feedback alone and both visual + haptic feedbacks available at the master site. **Results:** Surgical trainees' preference for the modality providing both visual and haptic feedback is corroborated by both quantitative and qualitative metrics. Hard nodules detection sensitivity improves ($94.35 \pm 9.1\%$ vs $76.09 \pm 19.15\%$ for visual feedback alone), while also exerting smaller forces (4.13 ± 1.02 N vs 4.82 ± 0.81 N for visual feedback alone) on the phantom tissues. At the same time, the subjective perceived workload decreases. **Conclusion:** Tissue-probe contact forces are estimated in a low cost and unique way, without the need of force sensors on the end-effector. Haptics demonstrated an improvement in the tumor detection rate, a reduction of the probing forces, and a decrease in the perceived workload for the trainees. **Significance:** Relevant benefits are demonstrated from the usage of combined cable-driven parallel manipulators and haptics during robotic minimally invasive procedures. The translation of robotic intraoperative palpation to

clinical practice could improve the detection and dissection of cancer nodules.

Index Terms—Surgical robotics, haptic feedback, cable-driven parallel robot, palpation, teleoperation, user study.

I. INTRODUCTION

HAPTIC sensation relates to the sense of touch and plays a crucial role in sensing – the perception of environmental information–, and manipulation – the active modification of the environment [1]. The sense of touch consists of a kinesthetic and a tactile component [2]. The kinesthetic information is fed back to muscles, tendons and joints as a reaction force whenever dynamic interactions with the environment occur. The tactile information is conveyed through specific nerve endings in the skin, known as mechanoreceptors, which detect shape, edges, temperature and texture of the probed object. Human touch perception is enabled by the kinesthetic-tactile synergy. Haptic devices, aimed at conveying the sense of touch to the human operator, have a wide variety of applications, ranging from space engineering, manufacturing and assembly, human-computer interaction for rehabilitation, prosthetics and surgical robotics [3].

When performing open surgeries, surgeons heavily rely on their sense of touch to discriminate blood vessels, nerves and tumors, which are usually harder than their surroundings [4]. Prostate, breast, thyroid, oral and ovarian cancers can be diagnosed at an early stage thanks to manual palpation [5], [8], which is performed by applying a varying pressure on a patient's superficial tissue. The rise of minimally invasive surgery in the 1980s stood for a real revolution in the operating room, enabling the surgeon to access target areas through small incisions and long, slender, laparoscopic instruments [9]. One of the main drawbacks of minimally invasive surgery is the impaired haptic perception caused by the interposition of laparoscopic tools between the surgeon's hands and the manipulated tissue, often forcing them to insert their fingers into access ports to retrieve tactile information [10]. Furthermore, the advent of robotics minimally invasive surgery has led to complete haptic sensory deprivation. This is the case for the majority of clinically used teleoperated master-slave systems, which cut-off force reflection from the surgeon site, forcing physicians to purely rely on visual cues to obtain critical information on tissue stiffness and deformation [11].

Manuscript received November 25, 2019; revised February 14, 2020; accepted April 1, 2020. Date of publication May 28, 2020; date of current version November 20, 2020. This work was supported in part by the NIHR Imperial Biomedical Research Centre (BRC) and in part by the ERANDA Rothschild Foundation. The work of George P. Mylonas was supported by the NIHR Imperial BRC. (Arianna Saracino and Timo J. C. Oude-Vrielink contributed equally to this work.) (Corresponding author: George P. Mylonas.)

Arianna Saracino is with the BioRobotics Institute, Scuola Superiore Sant'Anna, and also with the Center for Micro-BioRobotics@SSSA, Istituto Italiano di Tecnologia.

Timo J. C. Oude-Vrielink is with the Department of Surgery and Cancer, HARMS Lab, Imperial College London.

Arianna Menciassi is with the BioRobotics Institute, Scuola Superiore Sant'Anna.

Edoardo Sinibaldi is with the Center for Micro-BioRobotics@SSSA, Istituto Italiano di Tecnologia.

George P. Mylonas is with the Department of Surgery and Cancer and The Hamlyn Centre, HARMS Lab, Imperial College London, London SW7 2BU, U.K. (e-mail: george.mylonas@imperial.ac.uk).

Digital Object Identifier 10.1109/TBME.2020.2987646

Intracorporeal palpation for tumor detection relies on mechanical contrast-based discrimination between healthy and potentially cancerous tissues. Research on this topic is focused on the design of reliable, repeatable and real-time methods that will allow intracorporeal palpation - typically available in open surgery - in robotic minimally invasive procedures [12]. The two-fold nature of touch feedback gives rise to approaches tending more towards the force or the tactile components of the perception. Kinesthetic-based approaches [13], [14] are meant to apply forces and/or torque on the human hand to convey tool-tissue interaction forces and/or torque. Tactile-based approaches [15], [16] stimulate the skin using vibrations and/or pressure to recreate the contact sensation.

The need to restore the haptic sensation at the surgeon's site, while at the same time meeting clinical constraints and requirements, presents several technical challenges [17]. From an engineering standpoint, *sensor-based* and *sensor-less* approaches have been followed to measure tool-tissue interaction forces and render them to the surgeon's site.

Sensor-based approaches are based on the use of *tactile sensors* [18], [19], *haptic displays* [20] and *sensor-based palpation probes* [22], [23]. *Tactile sensors* and *haptic displays* mainly rely on cutaneous stimuli, perceived by mechanoreceptors in the human skin. The most encountered challenges for such systems are discussed in [18] and concern the translational aspects of these devices to clinical practice. The main limitations are pertinent to the small size of skin incisions during minimally invasive surgery procedures and to sterilization and biocompatibility issues, which are not negligible if the sensor is designed to be placed inside the patient's body. The need for integration with available surgical instruments must be considered as well. The main challenges for *sensor-based palpation probes* concern integration with available equipment and the conveyance of tissue mechanical properties to the clinicians, in an intuitive and real-time fashion.

On the other hand, *sensor-less* approaches usually rely on direct force feedback [24], [26]. In teleoperated systems, the slave robot is programmed to follow the master's motion as controlled by the human operator. When the user interface allows for both feedforward guidance of the slave and force feedback at the master site, the system becomes fully bidirectional and is often called bilateral [27]. Bilateral control architectures are employed to obtain direct force feedback, but their implementation imposes a trade-off between stability and haptic transparency [17], which is often used as a metric for the fidelity of the interaction rendering provided by the haptic device. *Sensor-less* approaches, e.g. based on motor currents for wrench estimation, can foster seamless integration into clinically relevant surgical robotic platforms [26], yet they are intrinsically less accurate in force rendering than *sensor-based* ones.

Despite the broad range of literature available on haptic feedback in surgery, an extensive user study involving subjects with medical background on a physical rather than virtual environment seems to be lacking. When dealing with intracorporeal palpation for tumor detection, most validation strategies involve users with non-medical background [11], [12], [20], [28]. To our knowledge, only [29] has presented an extensive user study,

involving 23 non-expert and 17 expert surgeons for the purpose of assessing haptic palpation benefits in a soft tissue simulation environment, based on a finite-element method. Additionally, only subjective metrics have been evaluated, based on measures obtained through Likert scale questionnaires. Compared to subjects with non-medical training, we strongly believe in the higher validity that subjects pursuing a career in surgery can offer when evaluating haptic perception for surgical palpation tasks. Such subjects have already undergone laparoendoscopic, and possibly robotic, training. For this study, resident physicians from level ST3 and above have been recruited. In the UK, ST3 level corresponds to the first of the specialists' years, after the first two years of core surgical training; their level corresponds to the third year of medical residency.

The work presented here discusses a new approach using a cable-driven parallel manipulator to provide haptic feedback to the surgeon. The use of a cable-driven parallel manipulator for manipulation of a surgical instrument has been first proposed with the CYCLOPS system in 2014 [30]. Advantages of the use of such systems are: efficient force transmission, a large and customizable workspace, and low end-effector inertia (thus high accelerations and velocities), as well as high positional accuracy and repeatability [31]. For flexible endoscopic therapeutic systems, when used for endoluminal or natural orifice transluminal endoscopic surgery procedures, low force exertion capability has been a major limitation for the translation to clinical practice [32]. The applicability of CYCLOPS as an attachment for flexible endoscopes has demonstrated the unique ability of the cable-driven parallel manipulator to exert forces up to 46 N, thus significantly facilitating procedures such as endoscopic submucosal dissection [33]. The relationship between end-effector forces and cable tensions can be also used inversely: forces on the end-effector can be estimated by measuring tension in the cables. For practical implementation of this in minimally invasive surgery, low friction is required while guiding the cables from proximal tension-sensing load cells near the motors, to the distally placed end-effector. One implementation of a cable-driven parallel manipulator as an instrument for the da Vinci (Intuitive Surgical Inc., Sunnyvale, CA, USA) surgical system has shown the ability to detect end-effector forces as low as 0.2 N [34]. This subsequently has allowed the performance of autonomous scanning of *ex vivo* liver tissue using confocal laser endomicroscopy.

The work presented in this paper uses the cable-driven parallel manipulator efficiency in force transmission to provide haptic feedback for intracorporeal soft tissue palpation. An earlier pilot study was carried out on a small sample of users ($n = 6$) with non-medical background. Technical discussions or benchmarking were not included in such pilot study [35]. This paper provides an in-depth technical description of the system's hardware and software. An initial benchmarking study is used to illustrate the accuracy of the system. A subsequent user study among 22 surgical trainees is used to provide quantitative and qualitative evaluation of the haptic feedback performance. Our focus concerns kinesthetic feedback rather than tactile. No tip-attached force/torque sensors are used to detect tool-tissue interaction forces, thus avoiding the related sterilization issues,

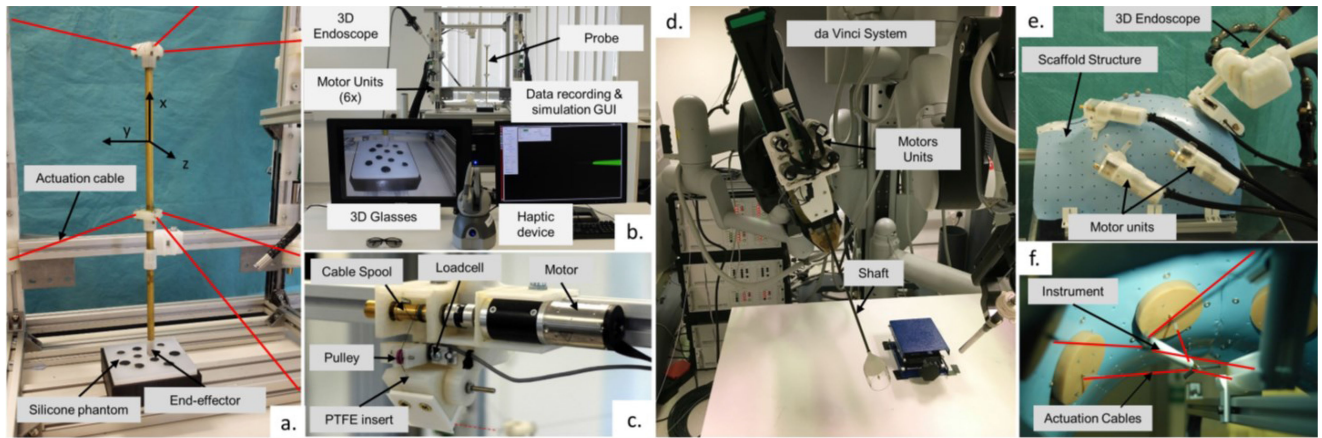


Fig. 1. (a), (b) and (c) show the CDAQS used as a slave system in this study: in (a) the end-effector is shown with cables enhanced in red for visualization purposes, (b) The complete experimental set-up: the Geomagic Touch haptic device as master system, the CDAQS as slave system, the 3D endoscope and its visualization screen, the control PC and corresponding screen used by the researchers to record the experimental data. (c) A close-up on one of the six motor units: the coupling between the motor and the cable is shown, as well as the position of the load cell, used to read the cable tension. (d), (e) and (f) show different configurations of the cable-driven parallel manipulator used in other studies. (d) A cable-driven parallel manipulator prototyped as a da Vinci surgical system end-effector for high accuracy tissue endomicroscopy [34]. (e) The SIMPLE prototype: the system uses a moldable outer scaffold structure placed over the insufflated abdomen. The motor units are mounted on the scaffold and needle ports are used as direct low friction pathways for the cable-driven parallel manipulator in the abdomen. (f) The view of one instrument of the SIMPLE system, showing the cable-driven parallel manipulator structure inside a simulated abdominal cavity.

and without increasing the size of the surgical instrument. Instead, forces are estimated in a cost-effective, simpler and easily adaptable way, using external load cells to measure cable tensions.

II. SYSTEM DESCRIPTION

The teleoperation setup comprises a Geomagic Touch haptic device (3D Systems, Rock Hill, USA) as master system, and a cable-driven parallel manipulator with force sensing capabilities as slave system (Fig. 1(a)–(c)). A 3D articulated endoscope (Endoeye Flex 3D, Olympus, Japan) was used for visualization purposes. The complete setup is shown in Fig. 1(b). This section details the system architecture, the inverse kinematics, the controller algorithm and the methods we used to calculate haptic forces to be conveyed at the master site. We then discuss the experimental evaluation of the system, which includes a technical benchmarking study realized through automatic raster scans, and a clinically oriented user study consisting of two teleoperated test-cases.

A. The CYCLOPS Data Acquisition System

Cable-driven parallel manipulators use a parallel configuration of cables to manipulate their end-effector. In general, as cables cannot be used for pushing, but only for pulling, the number of degrees of freedom is at least one less than the number of cables. The system used for the experimental evaluation and shown in Fig. 1(a)–(c) is referred to as CYCLOPS Data Acquisition System (CDAQS). An overview of the specifications is given in Table I. In this specific case, six cables allowed the end-effector to be controlled in five degrees of freedom. The CDAQS was specifically created for improvement and evaluation of core cable-driven parallel manipulator principles,

TABLE I
CDAQS SPECIFICATIONS

<i>End-effector</i>	Probe Length	300 mm
	Tip Diameter	8 mm
	Controllable Degrees of Freedom	x, y, z, yaw, pitch
<i>Cables</i>	Number of Cables	6
	Material	Spectra (UHMW PE)
	Diameter	0.19 mm
	Maximum Load	13 kgf
	Stiffness	3.1207 kNm
	Spool Diameter	9 mm
<i>Frame</i>	Frame Size	40x40x53 cm
	Workspace	14.6701 dm ³
<i>Motion scaling</i>	X, Y, Z	0.8

CYCLOPS Data Acquisition System (CDAQS) specifications. The dexterous workspace has been calculated by numerically integrating the Cartesian space of feasible poses for which an optimal tension distribution can be found.

before translating to a system optimized for a specific minimally invasive surgical procedure. The size of the CDAQS is larger than the aforementioned cable-driven parallel manipulators developed for minimally invasive surgery [33], [34]. However, most principles shown with CDAQS can be generalized and translated to the other smaller analogous surgical systems. For example, the motors used in the CDAQS have the same size and gear ratio as in systems with smaller workspaces. This affects the ability to scale the maximum velocity and acceleration of the system relative to scaffold size, with smaller systems being faster in this respect. Important to note is also the minimal friction in the CDAQS, using a direct pathway and PTFE tubing to route the cables from the motors to the end-effectors (see Fig. 1(b), (c)). Despite these two conditions for generalization, the current palpation study

does not concern maximum velocity and acceleration: it can thus be generalized to low friction, cable-driven parallel manipulator systems. A cable-driven parallel manipulator prototyped as a da Vinci instrument (shown in Fig. 1(d), [34]) and the SIMPLE system (Single-Incision MicroPort LaparoEndoscopic system, see Fig. 1(e), [36]), shown in previous studies, are examples of designs offering minimal friction. They can be compared to the CDAQS regarding their force sensing capabilities.

1) System Architecture: The length of each cable is controlled by rotating a 9 mm diameter cable spool connected to a brushless DC motor (2232S024BX4 with 22F 25:1 planetary gearheads, Faulhaber GmbH & Co.KG, Germany), coupled to an EtherCAT motion controller (MC 5004 P ET, Faulhaber GmbH & Co.KG, Germany). The EtherCAT slaves are connected in series and controlled by an EtherCAT master, over a 1Gbit ethernet cable at 1 kHz frequency. The EtherCAT master is a soft real-time Linux PC (Ubuntu 14.04, Canonical Ltd, UK. Real-time kernel patch 3.10.108). It is programmed in C++ with a GUI to update parameters and to record data for system's performance evaluation. The tension in the cables is read with a full-bridge single axis loadcell (LCL-020, Omega Engineering, Inc., Norwalk, CT, USA), connected to a digitizer (InstruNet i100, GW Instruments, Inc., Charlestown, MA, USA). The digitizer is only available in Windows Operating System: hence, a mini Windows computer (LattePanda, Shanghai, China) is used for collecting and transmitting the data over User Datagram Protocol to the Linux PC. The system is controlled by a Geomagic Touch haptic device, enabling force rendering in the three Cartesian degrees of freedom.

2) Inverse Kinematics: The inverse kinematics is related to the calculation of the motor joint space parameters in terms of the end-effector pose $\zeta = [x, y, z, \alpha, \beta, \gamma]$, where α, β, γ are yaw, pitch and roll angles respectively. The pose is related to the length of each cable, hence to the position of the cable attachment points on the end-effector p_i , and the points from which the cables act, or enter the scaffold, denoted as b_i . As the end-effector moves, the cable attachment points on the end-effector in the global coordinates $p_{i,g}$ are calculated from the local coordinate frame for a given pose:

$$p_{i,g} = \mathbf{R}(\alpha, \beta, \gamma) p_i + X, \quad (1)$$

where $\mathbf{R}(\alpha, \beta, \gamma)$ represents the rotation matrix for the given angles, and $X = [x, y, z]^T$ represents the global position vector of the end-effector's centre of motion. The vectors describing the cables can be expressed in matrix form as:

$$\mathbf{V}_m = \mathbf{B}_m - \mathbf{P}_{m,g}, \quad (2)$$

in which \mathbf{B}_m , $\mathbf{P}_{m,g}$ and \mathbf{V}_m contain respectively the scaffold entry points b_i , the attachment points in global coordinates $p_{i,g}$, and the cable vectors v_i for each cable $i = [1, \dots, n]$. The motor position q_i is calculated using the length of the cable vectors $v_{i,2}$ and the radius of the cable spool attached to the motor : $q_i = (v_{i,2} - v_{i,0,2})/\rho$, in which $v_{i,0}$ is the cable length at the calibration position.

The pose of the end-effector is also dependent on the static equilibrium of the cable tensions, and can be written as:

$$\mathbf{A}(\zeta) \vec{t} = \vec{w}, \quad (3)$$

For which \vec{t} is the vector containing the tension of all cables, and \vec{w} is the wrench vector containing the forces and moments acting on the end-effector. The so-called structure matrix $\mathbf{A}(\zeta)$ is pose dependent and it is the transpose of the Jacobian:

$$\mathbf{A}(\zeta) = \mathbf{J}^T = \begin{bmatrix} u_1 & \dots & u_n \\ u_1 \times p_{1,g} & \dots & u_n \times p_{n,g} \end{bmatrix}, \quad (4)$$

in which the rank of the structure matrix size is the number of controllable degrees of freedom m , ($\text{rank}(\mathbf{A}) = m = 5$), and its size depends on the number of cables n , $\mathbf{A} \in \mathbb{R}^{6 \times n}$. The normalized cable vectors $u_i = \frac{v_i}{v_i}$ are used as directional vectors for the cable tensions t_i .

3) Controller Algorithm: The control architecture is shown in Fig. 2. The controller comprises a PD-controller, based on measured and desired joint position q_i and velocity \dot{q}_i , and an additional controller to get the optimal cable tension distribution. The optimal tension distribution is important to keep the tensions sufficiently high to prevent cable slackness without exceeding their mechanical limits. Thus, each element of the tension vector \vec{t} must remain within a range of t_{min} and t_{max} , to prevent both cable slackness and failure:

$$\begin{aligned} \vec{t}_{opt} = \text{argmin} \|\mathbf{J}^T \vec{t} - (\vec{w}_{ext} + \vec{w}_g)\|_2 \\ \text{s.t. } t_{min} \leq t_i \leq t_{max}, \end{aligned} \quad (5)$$

in which the \vec{w}_g and \vec{w}_{ext} are the wrench vectors related respectively to the gravitational force and to other external forces, acting on the end-effector with respect to its centre of motion. The solution for the optimal tension distribution is solved online, using a bounded-variable least squares method [36], implemented in C++. Note that the solution of eq. (5) depends on the external wrench \vec{w}_{ext} . The equation can also be used to find the wrench-feasible workspace (i.e. the set of all poses ζ for which solutions that satisfy the tension conditions are found). When approaching the boundaries of the wrench-feasible workspace, the optimal solution provides null tension for at least one cable.

4) Calculation of the Haptic Forces: The probe-tissue contact forces can be estimated by modelling the end-effector as a free-floating object in space, and by calculating the force equilibrium to estimate forces acting on it. For each of the n cables we know the tension from the load cells and, in a deterministic fashion, for a given pose we know the orientation of each cable's force vector with respect to the end-effector. The force equilibrium equation hence becomes:

$$\sum_{i=1}^n \rightarrow F_i(\zeta, t_i) + \vec{F}_{ext} + \vec{F}_g + \mathbf{C} \dot{X} = \mathbf{M} \ddot{X}, \quad (6)$$

In which \mathbf{M} and \mathbf{C} are the mass and damping matrices, \vec{F}_g is the gravitational force, and \vec{F}_{ext} is an arbitrary external force acting on the end-effector. The cable force vectors $\rightarrow F_i(\zeta, t_i)$ can be calculated using the structure matrix, and can be written

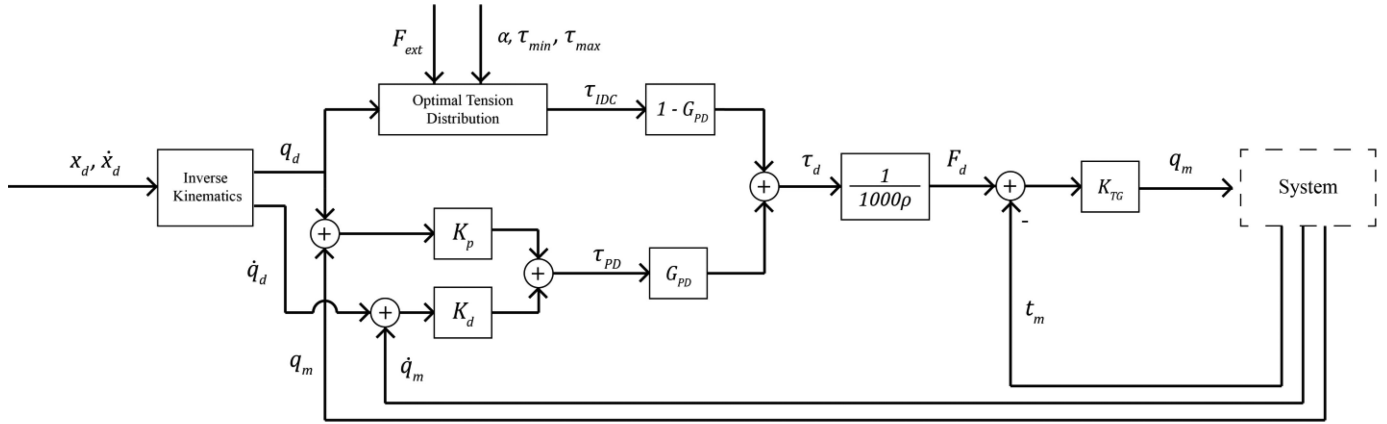


Fig. 2. Schematics of the control system responsible for the movements of the robotic end-effector. K_p and K_D are the gains of the PD-controller. The gain $G_{PD} \in [0, 1]$ balances the ratio of the optimal tension distribution and the PD-controller. The desired torque τ_D (mNm) is converted to desired tension F_D (N) using spool radius ρ , and compared with the measured cable tensions t_m . The tension gain K_{TG} is used to convert the force error to the commanded motor position q .

in matrix form as:

$$\sum_{i=1}^n \rightarrow F_i(\zeta, t_i) = \mathbf{U} \vec{t}_m \quad (7)$$

in which $\mathbf{U} \in \mathbb{R}^{3 \times n}$ comprises the top 3 rows of the structure matrix $A(\zeta)$, containing the cable unit vectors u_i , and \vec{t}_m contains the measured cable tensions $\vec{t}_m = [t_1, \dots, t_n]^T$. Inertia of cable-driven parallel manipulators is low, and we assume cable damping to be mostly accounted for by 1kHz control of the cable tension. Hence, leaving out damping and inertia, eq. (6) can be rewritten as:

$$\vec{F}_{ext} = -\vec{F}_g - \mathbf{U} \vec{t}_m. \quad (8)$$

To reduce noise in the estimation, a moving average is applied to each of the force measurements by the load cell; then, a second moving average is applied to the estimated force. As the implemented data connection between the loadcell's and the Linux PC poses a limitation on reading the frequencies of the cable tensions, the filter can only be applied over a small range of samples. Each cable tension measurement t_i is averaged over 10 samples before estimation of \vec{F}_{ext} . The estimated external force \vec{F}_{ext} is scaled down before being rendered by the haptic device. The force scaling is required to compensate for any effects on the perceived force caused by inaccuracies of the haptic device, the motion scaling from haptic device to the probe (see Table I) and latencies in the system. The scaling factor is determined heuristically by comparing the rendered force from the haptic device to a similar indentation performed manually with the same probe. When the perceived sensitivity with the haptic device was lower than when performed manually with the probe, the scaling factor was increased and vice versa. Factors such as the dynamic range of the device, the safety limits during the interaction with the operator, and the footprint of the end-effector on the probed tissue were also considered when choosing the scaling factor. The scaling factor was determined by the authors and was kept constant for all experiments and operators.

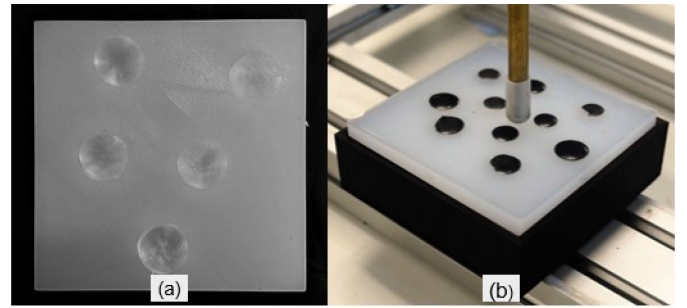


Fig. 3. (a) Top view of one of the silicone phantoms used for the user study. The soft matrix was realized with Ecoflex 00-30, while the five hard nodules, mimicking tumoral lumps, were made in Sylgard 184. We realized two identical phantoms, which only differed in the locations of the hard nodules. (b) The phantom was covered with a thin layer of Ecoflex 00-20 in correspondence of ten probing points, five of which corresponding to the hard nodules, before performing the user study. Participants were then instructed to only indent the phantom in correspondence of the black opaque dots.

III. EXPERIMENTAL VALIDATION

The main objective of this study was to evaluate the use of the CDAQS for intraoperative palpation. The current study used silicone phantoms for experimental evaluation, including both the system benchmarking and the actual palpation user study.

A. Silicone Phantoms

Three silicone phantoms of $20 \times 80 \times 80 \text{ mm}^3$ were made with mechanical properties simulating soft tissues (Fig. 3(a), (b)). The phantoms were created in-house with molds manufactured by additive manufacturing (PLA filament, Ultimaker 2+, Ultimaker BV, Netherlands). Each phantom was made of a soft base material (Ecoflex 00-30, Smooth-on, Inc., Macungie, USA), with five spheres of harder silicone (Sylgard 184, Dow Silicones Deutschland GmbH, Germany) hidden to simulate nodules [24], [38]. The Young's modulus of prostate cancer

tissue is reported to be about 200 kPa [38]: the mechanical properties of the used Sylgard 184 approximates this value. Ecoflex 00-30 is used in [24], as for healthy tissue a stiffness of roughly 10 times lower than tumors is expected (around 12–18 kPa, depending on the type of tissue). The nodules had a 15 mm diameter and were placed approximately 2 mm underneath the top surface. The top surface of the phantom had ten black opaque dots, created by adding black pigment to soft Ecoflex 00-20 material, and carefully depositing a thin layer on top of the cured phantom. The black dots were used to occlude any visual cues to the material below. Five of the black dots occluded the harder nodules, while the remaining five dots acted as distraction, and only had the homogeneous base material underneath their surface.

B. System Benchmarking

Benchmarking was conducted to investigate the accuracy of the estimated probe-tissue forces, to evaluate the system's behavior independently of the user, and to find the appropriate control conditions for the subsequent palpation user studies. This evaluation was carried out with an automatic raster scan of the silicone phantoms, using different indentation velocities and indentation depths. A 6 degrees of freedom load cell (Nano43, ATI Industrial Automation, Inc., Apex, NC, USA) was used below the silicone phantom to compare the estimated forces F_{est} to the ground truth forces. The real position of the end-effector was tracked using an optical tracking system ($2 \times$ Optitrack Prime 13W Cameras, NaturalPoint Inc, USA). Two additional phantoms were made from a single material to evaluate the system behavior on homogeneous material conditions. One phantom was created with the softer Ecoflex 00-30, and a second with Sylgard 184. The system was programmed to perform a linear indentation motion on the homogeneous silicone phantoms in different conditions. The indentation velocity is seen as a parameter that might influence the behavior and fidelity of force measurement [39]. Indentations at five different velocities were performed - [1, 5, 10, 20, 50] mm/s - to obtain a thorough characterization of the dynamic performance of the device. The indentation depth was taken as a third independent variable, and it was measured for automated indentations from 4 to 40 mm depth, allowing for generalization of the results to different indentations. During all experiments the tension in all cables T_m , the estimated force F_{est} , and the measured ground truth load F_{meas} were collected. The estimated force F_{est} was calculated online (eq. (8)), using the feed-forward desired position X_d . Eq. (8) was also used for the offline force estimation, referred to as $F_{est,comp}$, based on the real (tracked) end-effector position $X_{tracked}$. We calculated the ratio $r = F_{est}/F_{meas}$, which is a metric representing the accuracy of the estimation.

In addition, the system was validated on its ability to differentiate between the different stiffnesses of the silicone phantoms and of the hidden nodules. The raster scan involved a routine in which the surface area was split into a grid of 1225 palpation points, each at a 2 mm increment of the previous point. The raster scan indentation was performed at a velocity of 5 mm/s over a 6 mm depth. The motion speed between each palpation point was 20 mm/s.

C. User Study

We designed a user study to collect data during two palpation test-cases performed on the silicone phantoms. The first test-case assessed the ability of the participants to discriminate between different levels of stiffness based on haptic feedback alone: therefore, it will be referred to as the *Blind* palpation study. In the second test-case, possible haptic benefits in a task performed with and without force feedback were assessed: this test-case will be referred as the *Comparison* study. Each participant performed first the Blind study, then the Comparison study, and finally the Blind study again. The Blind study was performed once before the Comparison study to provide the investigators with a feedback of the haptic rendering fidelity, without the influence of vision. The repetition of the Blind study after the Comparison study was used to highlight possible effects between Blind's first and second trials, i.e. a user-confidence increase due to repeated uses of the system. The study was intentionally designed to fit within 30 minutes to prevent user fatigue. Before each trial, the probe was automatically sent to its homing position, corresponding to the center of the workspace. Each participant signed the informed consent form before starting the experiments. The experimental protocol (reference number: 18IC4524) was approved by the Joint Research Compliance Committee at Imperial College London.

1) Blind Palpation Experiment: During the Blind experiment, subjects were asked to focus entirely on the haptic rendering to detect any stiffness difference in the silicon phantom. No visual cues were available during this experiment. To facilitate blind palpation of different nodules on the silicone phantom, the haptic device motion was constrained to the indentation axis normal to the phantom surface. The investigator moved the phantom along a predefined path made of ten probing points, corresponding to the opaque black dots on the phantom surface. The investigator indicated when the phantom was repositioned, and the user was asked to probe the new position and to indicate whether it was soft or hard. Participants did not know how many hard nodules were embedded in the phantom. At any time during the experiment, the participant could ask for a reference probing, which always corresponded to soft matrix indentation.

2) Visual vs Visual + Haptics Comparison Experiment: Subjects experienced two different modalities while probing the soft phantom in search of hard inclusions:

- In the visual modality, users were provided with 3D visual feedback through the 3D endoscope mounted at the slave site; no haptic feedback was available.
- In the visual + haptics modality, users were provided with both 3D visual and haptic feedback at the same time.

Users were provided with 3D glasses during both modalities. Each user performed both modalities, and each one was performed twice to ensure repeatability on two silicone phantoms, which only differed in the nodules' location. The same two silicone phantoms were used for both modalities and for all users. To prevent learning bias, the starting modality was alternated per user: user#1 was asked to select the starting modality, and from user#2 onwards the initial modality was always switched. Similar to the Blind study, the users could ask for a reference

probing at any time, which would entail the probing of the soft surrounding phantom matrix.

3) Training and Indentation Technique: The participants spent approximately 5 minutes on a training session, to familiarize with the teleoperated system and the provided haptic feedback. During the first part of the training, free-space movements were performed to understand the master-slave mapping of the available degrees of freedom. Then, a trial silicone phantom with hard nodules embedded was used: the users were asked to probe the phantom by targeting the ten opaque black dots, and to detect the harder regions of the phantom corresponding to embedded nodules. Only five of the ten opaque black dots corresponded to hard nodules. The researcher, in this phase, would confirm the user's hypothesis regarding the presence or absence of a nodule. Subjects were given precise instructions to probe the silicone phantom through slow, controlled indentations, as this palpation technique is known to be preferable over continuous sliding. The work by Konstantinova et al. [40] on manual palpation strategies has underlined how subjects predominantly use normal force to detect hard nodule in soft phantoms, compared to lateral forces. In addition, LaMotte [41] has showed that, when the user is interacting with a real specimen through a stylus (same end-effector as the Geomagic Touch device that is used in this study), better inference about sample stiffness could be achieved by tapping on it, rather than applying a continuous pressure.

4) Performance Metrics: For both experiments, quantitative performance metrics were used to assess the impact of haptic integration with the CDAQS in terms of nodule detection rate, maximum indentation forces, and task completion time. The nodule detection rate is defined as the user's ability to discriminate tumor-mimicking hard nodules from the soft surrounding matrix. The maximum indentation forces are a metric to identify the users' exploration behavior on the silicone phantom.

For the Comparison experiment, complementary qualitative metrics were also considered, with the objective of comparing the users' feedback for the two experimental modalities. Subjective workload for both conditions was evaluated through two NASA-TLX questionnaires, provided to the users after completion of each condition. Lastly, subjects were given a Likert-scale questionnaire to determine their preference between the two presented conditions.

5) Participants: The user study was conducted on $n = 22$ recruited subjects (18 males, 4 females, average age 32 ± 1.9 years), all with medical background, from ST3 level and above, at St Mary's Hospital, London. None of the subjects declared any visual or other sensory deficiency.

6) Data Analysis: Depending on the nature of the evaluated variable (continuous or categorical), different statistical hypothesis tests were performed on Matlab (The Mathworks, Natick, MA, USA). For all cases, the significance level was set at 0.05.

For continuous variables in the experiments, namely maximum indentation forces and task completion time, we first applied a Shapiro-Wilk test to verify their normality. All data passed the normality check. Then, a repeated-measures t-test (or paired t-test) was performed to investigate the presence of any significant difference in the performance metrics between

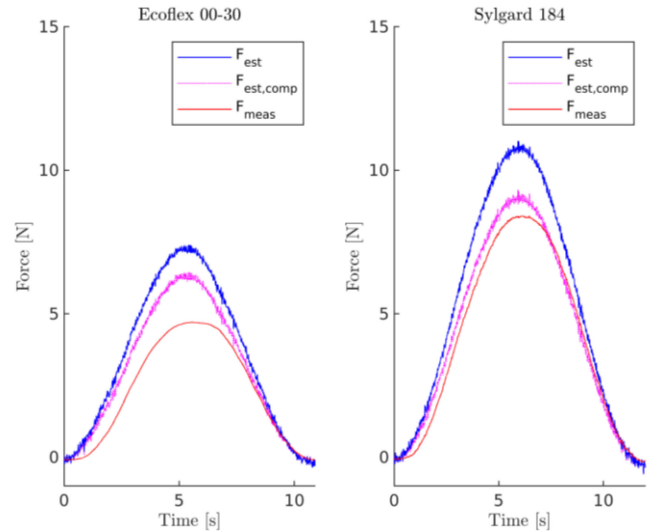


Fig. 4. Force estimation and ground truth force measurement of a single 6 mm deep indentation at a 1 mm/s indentation speed on two homogeneous material phantoms (Ecoflex 00-30 and Sylgard 184).

trial 1 and trial 2 in the Blind study, and the visual and visual + haptics modalities in the Comparison study.

For categorical variables, namely nodule detection rate and NASA-TLX scores, Wilcoxon signed-rank test was applied to assess differences between trial 1 and trial 2, or between visual and visual + haptic condition, respectively.

IV. RESULTS

A. System Benchmarking

The estimated forces F_{est} resulted higher than the measured forces F_{meas} , although with a similar force-profile. We found that the forces are estimated with an accuracy r of 1.38 and 1.64 for Sylgard 184 and Ecoflex 00-30, respectively, when indenting at a 1 mm/s speed (Fig. 4). When the end-effector is tracked and compensated for positional errors, the estimation accuracy increases (see $F_{est,comp}$ in Fig. 4). Both the measured and estimated forces decrease at higher indentation velocities (Fig. 5). However, the ratio r , a measure for the accuracy of the force estimation, remains relatively stable for all velocities. The indentation depth had some influence on the accuracy, in particular at shallower indentations. More specifically, the estimated forces remained higher than the measured forces for all indentation depths, though they flattened out when the indentation increased (Fig. 6). Cable slackness occurred at large indentations, as encircled in Fig. 6, however, no considerable changes in the estimation accuracy occurred. The raster scans obtained from the automated benchmarks on two silicone phantoms with embedded hard nodules are shown in Fig. 7(a), (b).

B. User Study

1) Blind Palpation Experiment: Nodule detection sensitivity across the two trials exceeded 70% (Fig. 8: $70.9 \pm 16.01\%$ and $77.27 \pm 22.51\%$ for trial 1 and 2, respectively). Wilcoxon

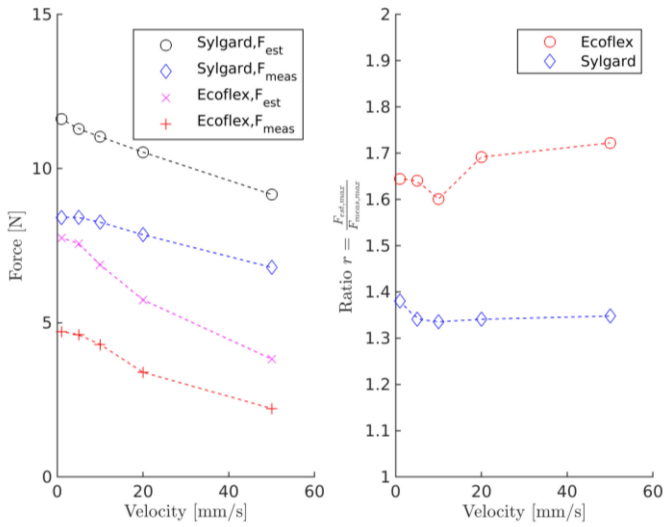


Fig. 5. The estimated and measured force while indenting the Sylgard and Ecoflex plain phantom.

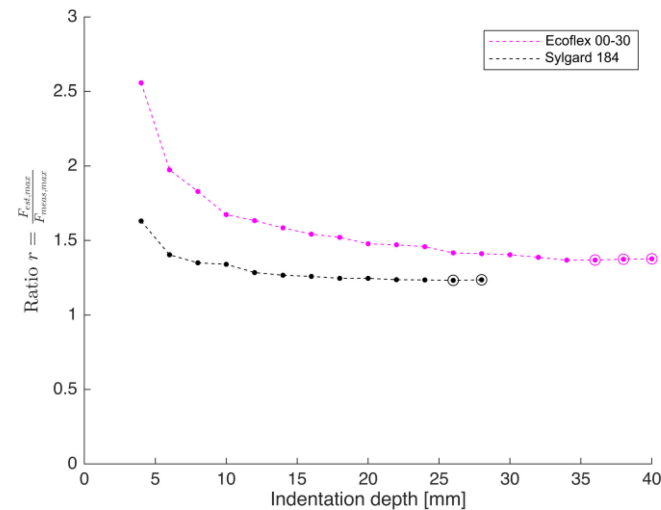


Fig. 6. The ratio r at different indentation depths, conducted on both the Sylgard and Ecoflex silicone phantoms. The encircled data points are points at which at least one cable exhibits slackness: however, no change in estimation accuracy occurs.

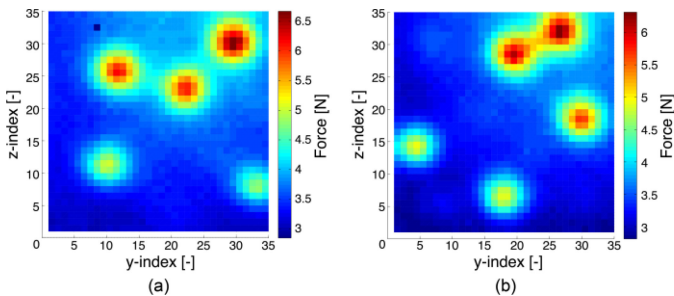


Fig. 7. The force-maps of the raster scans performed on the two silicone phantoms used during the user studies. The hard silicone nodules are visible through the higher estimated indentation forces.

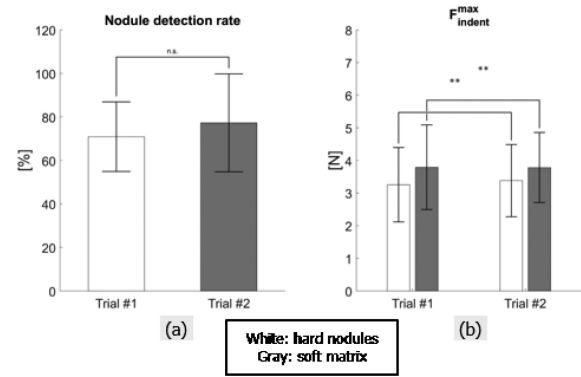


Fig. 8. The nodule detection rate and maximum indentation force of both Blind palpation trials, the first before and the second after the Comparison study. (a) The nodule detection rate was not significantly different between both blind trials. (b) The maximum indentation forces differed between both blind trials on both the soft matrix and the hard nodules.

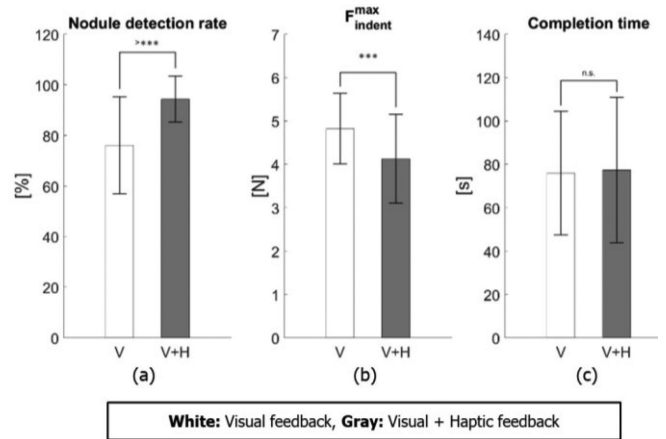


Fig. 9. (a) The nodule detection rate was significantly different for the haptic trials compared to the visual-only trials. (b) The maximum indentation forces were significantly different. (c) The task completion time was not significantly different.

signed rank test, however, revealed no significant difference between the trials ($Z = -1.16$, $p = 0.25$).

On the soft silicone matrix maximum indentation forces of 3.38 ± 1.11 N and 3.78 ± 1.07 N were found for trials 1 and 2, respectively (Fig. 8(b)). On the hard nodules, forces of 3.25 ± 1.14 N and 3.79 ± 1.29 N were found, respectively. Higher forces were applied during trial 2 with respect to trial 1 on both tissues. The repeated measures t-test revealed a statistically significant difference between the two trials in the probing (hard nodules: $t(18) = -3.29$, $p = 0.0041$, soft matrix: $t(18) = -3.05$, $p = 0.0069$).

2) Visual vs. Visual + Haptics Comparison experiment:

The users detected a higher number of hard inclusions when haptic feedback was available. Additionally, with haptic feedback the nodule detection rate was significantly different than when the task was performed with visual feedback alone (Fig. 9(a): $94.35 \pm 9.1\%$ visual + haptics versus $76.09 \pm 19.15\%$ visual only; Wilcoxon signed-rank test results: $Z = -4.5$, $p < 0.0001$).

TABLE II
LIKERT SCALE QUESTIONNAIRE RESULTS

Question #	SD [%]	D [%]	N [%]	A [%]	SA [%]
1. I was feeling more comfortable using the system with force feedback	/	10	10	62	19
2. The task was easier to perform with force feedback than without force feedback	/	5	14	48	33
3. The task with force feedback was less stressful than without force feedback	/	14	33	38	14
4. Overall, I would choose to have force feedback than not having force feedback	/	10	5	48	38

The questionnaire was presented to the subjects at the end of the Comparison experiment. These qualitative results refer to the comparison between visual and visual + haptics modalities. SD: strongly disagree, D: disagree, N: neutral, A: agree, SA: strongly agree

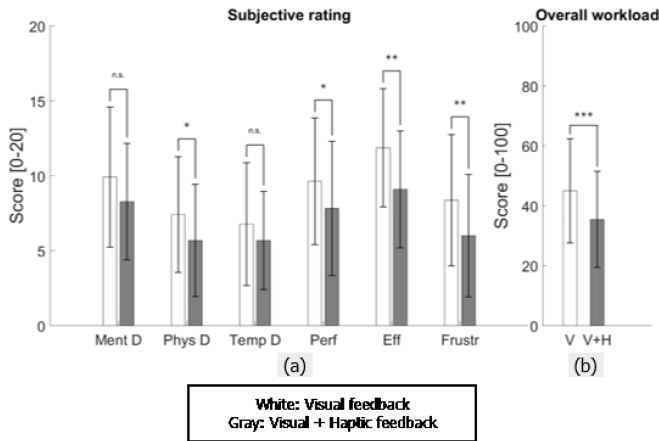


Fig. 10. The qualitative results from the NASA-TLX questionnaire during the Comparison experiment. A score range is set from 0 to 20: higher scores corresponded to a higher perceived workload. (a) Single factors: Mental Demand, Physical Demand, Temporal Demand, Performance, Effort, Frustration. (b) Overall workload over all factors shows a significantly different perceived workload between the visual and the visual + haptic modalities.

When provided with haptics in addition to visual feedback, the users applied smaller forces on the phantom surface. The maximum indentation force for haptic feedback was 4.13 ± 1.02 N, compared to a 4.82 ± 0.81 N for visual feedback alone (Fig. 9(b)), demonstrating a statistically significant difference with the repeated-measures t-test ($t(21) = 4.34$, $p = 0.0003$).

As for the task completion time, no statistically significant difference was shown ($t(20) = -0.25$, $p = 0.8$) between the two modalities and the variances were high in both cases. The task completion time was 75.95 ± 28.5 s and 77.36 ± 33.46 s for the visual-only and haptic experiments, respectively (Fig. 9(c)).

3) Qualitative Assessment: The qualitative assessment through NASA-TLX questionnaires showed a lower perceived effort, frustration and physical demand when haptic feedback was active. The users also predicted to have performed better with haptics (Fig. 10(a)). Wilcoxon signed-rank test detected statistically significant differences between the visual and visual + haptic modalities for the following single factors: physical demand ($Z = 2.55$, $p = 0.011$), performance ($Z = 1.97$, $p = 0.049$), effort ($Z = 3.05$, $p = 0.002$), and frustration ($Z = 2.68$, $p = 0.0074$).

These results were further confirmed by the NASA-TLX overall workload score (Fig. 10(b)). The subjective perceived workload during the Comparison experiments was significantly

lower when haptics was available to the user. Wilcoxon signed-rank test revealed a statistically significant difference between the two conditions ($Z = 3.36$, $p = 0.0008$).

Likert scale questionnaire results (Table II) further corroborate the users' qualitative preference for the presence of haptic feedback during the experiments.

V. DISCUSSION

The main objective of this work was to evaluate the performances of a teleoperated cable-driven parallel manipulator with force sensing capabilities, to be applied in intracorporeal palpation for tumor detection. We focused on kinesthetic haptic feedback rather than tactile one, as this setup is easier to be integrated in existing platforms. We did not use any tip-attached force sensor, therefore avoiding sterilization issues and reducing costs. Instead, contact forces were estimated through external load cells that measure cable tensions.

We demonstrated that delivering haptic feedback to the users (1) improved the tumor detection rate, (2) decreased the applied forces on the tissues, and (3) diminished the perceived workload for the surgical trainees involved in the study.

A. Benchmarking

The benchmarking studies showed that indentation forces can successfully be used to differentiate between different stiffnesses. This is shown in plain silicone phantoms of different hardness, as well as in phantoms with integrated nodules. The force estimation still deviates from the absolute force measurement. For user control, such absolute force estimation is less important than the relative force estimation, especially if the order of magnitude is correct [42]. The benchmarking studies showed that the accuracy also remained stable independently of the indentation velocity.

Various technical aspects have to be considered when interpreting the benchmarking studies we performed on the CDAQS. Cable slackness is known to be a problem for controllability of robotic systems, especially for those with single redundancy (e.g. CDAQS with 5 degrees of freedom and 6 tendons). However, the current study on the CDAQS showed that the force estimation was not compromised by the presence of slack cables. Additionally, it has been observed that the end-effector pose does not drastically change after slackness. Therefore, the static equilibrium of eq. (6) holds, and the slackness is predominantly a result of the normal behaviour of the cable-driven parallel manipulator, i.e. the system is operating at the boundaries of

the wrench-feasible workspace (as mentioned in Section IIA.3). The slackness is thus predictable using eq. (5).

On a more general note, we also want to emphasize the different origin for slackness in cable-driven serial and parallel manipulators. While in serial mechanisms the slackness is caused by a combination of cable elasticity and highly non-linear friction in the cables, parallel mechanisms are less prone to these effects in two different ways. Firstly, forces on the end-effectors are distributed among all the actuators, therefore requiring less force per actuator, which in turn results to lower elongation and friction at each cable. For cable-driven serial mechanisms, in contrast, high cable forces are required due to an unfavourable transmission ratio related to the small joints, the relatively long arms, and cumulative effect of forces; the lowest joint in a serial mechanism gets the highest moments. Secondly, in cable-driven parallel manipulators the motions in the cables are generally more directly related to the motion of the end-effector. For cable-driven serial mechanisms, the unfavourable transmission ratio also affects the motions; small motions of the cable are converted to large motions in the end-effector space. As a result, a small error caused by elongation or friction is amplified, and for multiple links this error accumulates. Thus, in short, the more favourable transmission ratio of cable-driven parallel mechanisms reduce both the magnitude and the effect that elongation and friction has on the end-effector. This effect is diminished to such an extent that it is not the main source of slackness in our system and, as demonstrated in this paper, that cable tensions can successfully be used to estimate the end-effector forces.

Even though the results show that cable slackness does not hinder the estimation of the forces, slippage at the tissue-tip interface may result in a sudden change in pose when one or more cables are slack, and thereby influencing the estimated forces. While this is an important issue to consider in further developments, it should be noted that, during the benchmarking study, the slackness only occurred with high external forces. Such forces may lie outside the limits of safe tissue handling, therefore, should ideally be restrained within safety limits imposed by software.

The absolute force accuracy will be important for surgical robotic systems performing (semi-) autonomous, force-based tasks, such as palpation. While manual palpation is an alternative, the automation of a repetitive task may reduce the cognitive load for the surgeon. In such applications, the absolute force estimation becomes important, not only for the accuracy of the task itself, but also for safety. The absolute accuracy of the current system deviates still too much for such applications: however, there are reasons to believe that the absolute accuracy of the system can be further increased due to the simplicity of the current force estimation. The force estimation method can be expanded by including cable elasticity and friction models [43], [44]. When considering force vectors $\rightarrow F_i(\zeta, t_i)$ in eq. (6), the friction decreases both the accuracy of the cable tension measurement t_i and the cable elasticity the accuracy of pose ζ . The cable pretension is an important aspect that influences the friction within the system. As the end-effector stiffness is also directly related to the cable (pre-) tension [45], an active stiffness controller to set the stiffness at a minimum level will

further increase the absolute accuracy. A reduced friction would also contribute to a higher accuracy at smaller indentations, thus resulting in a lower sensitivity threshold. That is because these indentations are influenced mostly by the relative effect of the pretension, rather than external forces. Another improvement of the model is tracking the end-effector position while in use. The current estimation method is based on a deterministic assumption regarding the position of the end-effector. However, in practice its position under external loads deviates from the feed-forward position. This is an effect of the overall end-effector stiffness as a combination of control stiffness and cable stiffness. Using the tracked pose instead of the feed-forward pose has shown to improve the force estimation ($F_{est,comp}$ in Fig. 4). Hence, the implementation of online end-effector tracking methods, either through measurement or estimation [46], will further increase the accuracy. The usage of the tracked pose for the force estimation has not been implemented in the current user study, as the cable-driven parallel manipulator prototypes in minimally invasive surgery do not have this capability yet.

B. User Study

For the Blind palpation study, in which users had to detect hard nodules without any visual cue, we can deduce that there was not a specific learning effect correlated to the success rate. Users may have been influenced by the fact that trials 1 and 2 were separated by the Comparison experiment, in which visual feedback was always available. However, the reported detection sensitivity in trial 1 was over 70%, and this trend slightly increased in trial 2. In [6], authors performed a blind palpation test to compare the performances of the human finger to those of a tactile sensor. The sensor outperformed the finger for superficial tumors (up to 3 mm depth), in terms of detection rate (94.1% vs 87.6%). Such high performance in a blind test can be attributed to the tactile nature of the device. In contrast, our system provides kinesthetic feedback. Users exerted higher forces during trial 2, which can bring evidence for a higher confidence level during the whole experimental procedure. The latter result could encourage more long-term user studies in the future. Haptic cues would enrich the surgeons' training phase, and potential related benefits could be assessed.

With the Comparison study, the two most striking claims of this work are highlighted. The palpation task, in which visual and visual + haptic modalities were compared, proves that the availability of haptic feedback resulted in an increase in nodule detection sensitivity, and a reduction in the magnitude of the applied forces. These results signify improved diagnostic accuracy and reduced damage of the targeted and surrounding tissues during intraoperative robotic palpation. Improved accuracy [47] and decreased applied forces [48] have also been valued as haptic feedback benefits in other surgical tasks, such as dissection, suturing, and in more complex tasks, e.g. teleoperated laparoscopy for endometriosis surgery [49]. Other research has provided similar evidence using the direct force feedback approach for palpation [17]. The study has showed minimized detection errors when visual and force feedback are combined, compared to visual feedback alone, but the platform in use suffered from

the typical transparency issues present in direct force feedback platforms.

The qualitative results are coherent with the quantitative ones, as a clear preference for the haptic feedback modality emerged. NASA-TLX overall score was found significantly lower in visual + haptic condition, which signifies a lower perceived workload in presence of the force reflection at the master site. Single factors, such as physical demand, performance, effort and frustration, equally attested to the superiority of the haptic condition. This evidence visibly points towards a clear user preference for the presence of haptic feedback. Users performed better when haptic feedback was available, as the detection sensitivity was higher in that modality. Moreover, lower effort and frustration are very important aspects for the clinical applicability of haptic technologies. These findings were supported by the Likert scale results as well.

The lack of palpation studies involving subjects with a clinical background [6], [17] has been reported as a limiting factor. In the work presented here, we only recruited subjects with clinical background (ST3 and above, $n = 22$), and this represents a key aspect that gives further validity to our study. This claim is corroborated by the results obtained in our previous work [35]. It involved $n = 6$ subjects with engineering background, who performed a tumor detection task, analogous to the one performed in the Comparison experiment in this manuscript. Results showed that no statistically significant quantitative differences existed between their performance in the visual and visual + haptic modalities. On the other hand, qualitative metrics clearly underlined user preferences for the visual + haptic condition. Those contradictory findings were obtained considering a much smaller sample-size of participants ($n = 6$), none of which had any clinical background.

In future work, we will address the clinical translation of our platform, targeting all the related issues which could affect haptic transparency and fidelity. To do so, the feedback collected from surgical trainees at the end of each experimental session will be considered. Some users would have preferred a longer training time: we never exceeded 10 minutes training time, as our intention was to keep the total duration of the experiment within 30 minutes. Some trainees that received laparoscopic but not robotics training in their career, commented that they would have liked to have more experience with 3D vision, and with instruments motions which are, in contrast to laparoscopy, not inverted through the pivoting around a trocar. In addition, the platform will be evaluated in more realistic environments, i.e. *ex vivo* tissue trials, and trials involving nodules at variable depths.

Clinical translation of this work will require further studies to be performed on one of the already developed low-friction cable-driven parallel manipulator prototypes, such as the da Vinci CYCLOPS Instrument and SIMPLE (see Section IIA and Fig. 1(e)–(f)). SIMPLE, with 6 cables to control 5 degrees of freedom and designed for the abdomen, resembles the CDAQS the most in terms of configuration and size. In contrast, the da Vinci CYCLOPS Instrument is a small-scale and planar (3 degrees of freedom) system, and its force estimator was set-up only for the planar system. The force estimator described in the current paper can be used for any arbitrary number of cables and

sizes: therefore, it can be applied to both prototypes without any change. We expect that the findings in the current paper can be adopted for intracorporeal palpation in other systems with low friction.

VI. CONCLUSION

This paper introduced a new, simple and cost-effective approach for restoring the sense of touch during intracorporeal palpation, using a teleoperated cable-driven parallel manipulator, namely the CDAQS. The performance of the CDAQS has been evaluated with a preliminary technical benchmarking, and with a clinically oriented user study, involving $n = 22$ surgeons in training. To the authors' knowledge, such an extensive study was lacking in the haptic palpation domain. The benchmarking tests showed evidence of good absolute accuracy of our force estimation method, despite its simplicity. The CDAQS capability to differentiate objects of different stiffness was not altered by velocity changes or cable slackness. Other key features of our system are the scalability and the lack of proximal sensors, which make the sensing technique unique and easy to be incorporated in existing systems, as previously demonstrated in [34]. Our multifaceted key outcomes highlight the potential benefits brought by haptic feedback restoration in robotic minimally invasive surgery. When the haptic feedback was available to the users, the experiments proved (1) an increased detection of superficial nodules, (2) a reduction of indentation forces applied on the tissue, which could lead to a decrease in healthy tissue damage during intraoperative palpation procedures, and (3) a decreased subjective workload perceived by the trainees.

The proposed system is nearly ready for real surgery; the remote sensing strategy avoids end-effector tip-attached sensors, it is easy to be replicated, seamlessly and cost-effectively. The reported findings may help to bring intraoperative palpation from open surgery to minimally invasive teleoperated surgery, facilitating tumor detection with touch, leading to significant improvements in early diagnosis of cancer.

ACKNOWLEDGMENT

The authors would like to thank Prof. Ferdinando Rodriguez y Baena and Eloise Matheson from the Mechatronics in Medicine Lab, Imperial College London for using their Nano43 loadcell during the benchmarking study.

REFERENCES

- [1] A. E. Saddik *et al.*, "Haptics: General principles," in *Haptics Technologies. Springer Series on Touch and Haptic Systems*. Berlin, Germany: Springer, 2011, pp. 1–20.
- [2] A. M. Okamura, "Haptic feedback in robot-assisted minimally invasive surgery," *Current Opinion Urol.*, vol. 19, no. 1, pp. 102–107, 2009.
- [3] B. Hannaford and A. M. Okamura, "Haptics," in *Handbook of Robotics*. Berlin, Germany: Springer, 2008, pp. 719–739.
- [4] A. Manduca *et al.*, "Magnetic resonance elastography: Non-invasive mapping of tissue elasticity," *Med. Image Anal.*, vol. 5, no. 4, pp. 237–254, 2001.
- [5] M. J. Roobol, "Digital rectal examination can detect early prostate cancer," *Evid. Based Med.*, vol. 20, no. 3, pp. 119–119, 2015.
- [6] M. Sharon *et al.*, "Performance and reporting of clinical breast examination: A review of the literature," *CA Cancer J. Clin.*, vol. 54, no. 6, pp. 345–361, 2004.

- [7] J. L. Gray *et al.*, "Routine thyroglobulin, neck ultrasound and physical examination in the routine follow up of patients with differentiated thyroid cancer—Where is the evidence?" *Endocr. J.*, vol. 62, no. 1, pp. 26–33, 2018.
- [8] M. Droudi *et al.*, "The bimanual ovarian palpation examination in the Prostate, Lung, Colorectal and Ovarian cancer screening trial: Performance and complications," *J. Med. Screen.*, vol. 24, no. 4, pp. 220–222, 2017.
- [9] D. B. Camarillo *et al.*, "Robotic technology in surgery: Past, present, and future," *Amer J. Surgery*, vol. 188, no. 4, pp. 2–15, 2004.
- [10] M. S. Arian *et al.*, "Using the BioTac as a tumor localization tool," in *Proc. IEEE Haptics Symp.*, 2014, pp. 443–448.
- [11] M. E. Hagen *et al.*, "Visual clues act as a substitute for haptic feedback in robotic surgery," *Surgical Endoscopy*, vol. 22, no. 6, pp. 1505–1508, 2008.
- [12] M. Li *et al.*, "Intra-operative tumour localisation in robot-assisted minimally invasive surgery: A review," *Proc. Inst. Mech. Engineers, Part H*, vol. 228, no. 5, pp. 509–522, 2014.
- [13] A. Filippeschi *et al.*, "Encountered-type haptic interface for virtual interaction with real objects based on implicit surface haptic rendering for remote palpation," in *Proc. IEEE Int. Conf. Robot. Syst.*, 2015, pp. 5904–5909.
- [14] J. Konstantinova *et al.*, "Evaluating manual palpation trajectory patterns in tele-manipulation for soft tissue examination," in *Proc. IEEE Int. Conf. Cybern.*, 2013, pp. 4190–4195.
- [15] C. R. Wottawa *et al.*, "Evaluating tactile feedback in robotic surgery for potential clinical application using an animal model," *Surgical Endoscopy*, vol. 30, no. 8, pp. 3198–3209, 2015.
- [16] T. Fukuda *et al.*, "Visual and tactile feedback for a direct-manipulating tactile sensor in laparoscopic palpation," *Int. J. Med. Robot. Comp.*, vol. 14, no. 2, 2018, Art. no. e1879.
- [17] N. Enayati, E. D. Momi, and G. Ferrigno, "Haptics in robot-assisted surgery: Challenges and benefits," *IEEE Rev. Biomed. Eng.*, vol. 9, pp. 49–65, Mar. 2016. [Online]. Available: <https://ieeexplore.ieee.org/abstract/document/7425205>
- [18] C. Pacchierotti, D. Prattichizzo, and K. J. Kuchenbecker, "Cutaneous feedback of fingertip deformation and vibration for palpation in robotic surgery," *IEEE Trans. Biomed. Eng.*, vol. 63, no. 2, pp. 278–287, Feb. 2016.
- [19] J. Konstantinova *et al.*, "Implementation of tactile sensing for palpation in robot-assisted minimally invasive surgery: A review," *IEEE Sens. J.*, vol. 14, no. 8, pp. 2490–2501, Aug. 2014.
- [20] R. Rizzo, A. Musolino, and L. A. Jones, "Shape localization and recognition using a magnetorheological-fluid haptic display," *IEEE T. Haptics*, vol. 11, no. 2, pp. 317–321, Apr.–Jun. 2018.
- [21] M. Beccani *et al.*, "Wireless tissue palpation for intraoperative detection of lumps in the soft tissue," *IEEE Trans. Biomed. Eng.*, vol. 61, no. 2, pp. 353–361, Feb. 2014.
- [22] S. McKinley *et al.*, "A single-use haptic palpation probe for locating subcutaneous blood vessels in robot-assisted minimally invasive surgery," in *Proc. IEEE Int. Conf. Autom. Sci. Eng.*, 2015, pp. 1151–1158.
- [23] A. Faragasso *et al.*, "Real-time vision-based stiffness mapping," *Sensors*, vol. 18, no. 5, 2018, Art. no. 1347.
- [24] J. C. Gwilliam *et al.*, "Effects of haptic and graphical force feedback on teleoperated palpation," in *Proc. IEEE Int. Conf. Robot. Autom.*, 2009, pp. 677–682.
- [25] M. Mahvash *et al.*, "Force-feedback surgical teleoperator: Controller design and palpation experiments," in *Proc. Symp. Haptic Interfaces Virtual Environ. Teleoperator Syst.*, 2008, pp. 465–471.
- [26] A. Saracino *et al.*, "Haptic feedback in the da Vinci Research Kit (dVRK): A user study based on grasping, palpation, and incision tasks," *Int. J. Med. Robotics Comput. Assisted Surgery*, vol. 15, no. 4, 2019, Art. no. e1999.
- [27] G. Niemeyer, C. Preusche, and G. Hirzinger, "Telerobotics," in *Handbook of Robotics*. Berlin, Germany: Springer, 2008, pp. 741–758.
- [28] C. Pacchierotti *et al.*, "Cutaneous haptic feedback to ensure the stability of robotic teleoperation systems," *Int. J. Rob. Res.*, vol. 34, no. 14, pp. 1773–1787, 2015.
- [29] S. Ullrich and T. Kuhlen, "Haptic palpation for medical simulation in virtual environments," *IEEE Trans. Visualization Comput. Graph.*, vol. 18, no. 4, pp. 617–625, Apr. 2012.
- [30] G. P. Mylonas *et al.*, "CYCLOPS: A versatile robotic tool for bimanual single-access and natural-orifice endoscopic surgery," in *Proc. IEEE Int. Conf. Robot. Autom.*, 2014, pp. 2436–2442.
- [31] C. Gosselin, "Cable-driven parallel mechanisms: State of the art and perspectives," *Mech. Eng. Rev.*, vol. 1, no. 1, 2014, Art. no. DSM0004.
- [32] V. Vitiello *et al.*, "Emerging robotic platforms for minimally invasive surgery," *IEEE Rev. Biomed. Eng.*, vol. 6, pp. 111–126, Dec. 2013. [Online]. Available: <https://ieeexplore.ieee.org/abstract/document/7425205>
- [33] T. J. Oude-Vrielink *et al.*, "ESD CYCLOPS: A new robotic surgical system for GI surgery," in *Proc. IEEE Int. Conf. Robot. Autom.*, 2018, pp. 150–157.
- [34] K. Miyashita *et al.*, "A cable-driven parallel manipulator with force sensing capabilities for high-accuracy tissue endomicroscopy," *Int. J. Comput. Assist. Radiol. Surg.*, vol. 13, no. 5, pp. 659–669, 2018.
- [35] A. Saracino *et al.*, "Haptics-enabled palpation for intraoperative tumour detection using a cable-driven parallel manipulator," in *Proc. Joint Workshop New Techn. Comput. Robot Assist. Surgery*, 2018, pp. 71–72.
- [36] T. J. C. Oude-Vrielink *et al.*, "A Simple surgical robot concept: a bimanual single-port system with intrinsic force-sensing capability," in *Proc. Joint Workshop New Techn. Comput. Robot Assist. Surgery*, 2018, pp. 57–58.
- [37] P. B. Stark and R. L. Parker, "Bounded-variable least-squares: An algorithm and applications," *Comp. Stat.*, vol. 10, no. 2, pp. 129–129, 1995.
- [38] B. Ahn *et al.*, "New approach for abnormal tissue localization with robotic palpation and mechanical property characterization," in *Proc. IEEE Int. Conf. Robot. Syst.*, 2011, pp. 4516–4521.
- [39] J. Konstantinova *et al.*, "Force-velocity modulation strategies for soft tissue examination," in *Proc. IEEE Int. Conf. Robot. Syst.*, 2013, pp. 1998–2003.
- [40] J. Konstantinova *et al.*, "Palpation force modulation strategies to identify hard regions in soft tissue organs," *PLOS ONE*, vol. 12, no. 2, 2017, Paper e0171706.
- [41] R. H. LaMotte, "Softness discrimination with a tool," *J Neurophysiol.*, vol. 83, no. 4, pp. 1777–1786, 2000.
- [42] L. A. Jones, "Perception of force and weight: Theory and research," *Psych. bulletin*, vol. 100, no. 1, pp. 29–42, 1986.
- [43] P. Miermeister *et al.*, "An elastic cable model for cable-driven parallel robots including hysteresis effects," in *Cable-Driven Parallel Robots*. Berlin, Germany: Springer, 2015, pp. 17–28.
- [44] V. Agrawal, W. J. Peine, and B. Yao, "Modeling of transmission characteristics across a cable-conduit system," *IEEE Trans. Robot.*, vol. 26, no. 5, pp. 914–924, Oct. 2010.
- [45] S. Behzadipour and A. Khajepour, "Stiffness of cable-based parallel manipulators with application to stability analysis," *J. Mech. Design*, vol. 128, no. 1, pp. 303–310, 2006.
- [46] G. Pittiglio *et al.*, "Dynamic control of cable driven parallel robots with unknown cable stiffness: A joint space approach," in *Proc. IEEE Int. Conf. Robot. Autom.*, 2018, pp. 948–955.
- [47] L. Moody *et al.*, "Objective surgical performance evaluation based on haptic feedback," *Stud. Health. Technol. Inform.*, vol. 85, pp. 304–310, 2002.
- [48] C. R. Wagner *et al.*, "The role of force feedback in surgery: Analysis of blunt dissection," in *Proc. 10th Symp. Haptic Interfaces Virtual Environ. Teleop. Syst.*, 2002, pp. 68–74.
- [49] S. J. P. Diez *et al.*, "Evaluation of haptic feedback on bimanually teleoperated laparoscopy for endometriosis surgery," *IEEE Trans. Biomed. Eng.*, vol. 66, no. 5, pp. 1207–1221, May 2019.